ISSN 1063-7834, Physics of the Solid State, 2018, Vol. 60, No. 5, pp. 1021–1028. © Pleiades Publishing, Ltd., 2018.
Original Russian Text © V.A. Terekhov, D.S. Usol'tseva, O.V. Serbin, I.E. Zanin, T.V. Kulikova, D.N. Nesterov, K.A. Barkov, A.V. Sitnikov, S.K. Lazaruk, E.P. Domashevskaya, 2018, published in Fizika Tverdogo Tela, 2018, Vol. 60, No. 5, pp. 1005–1011.

SURFACE PHYSICS AND THIN FILMS

Phase Formation and Electronic Structure Peculiarities in the $Al_{1-x}Si_x$ Film Composites under the Conditions of Magnetron and Ion-Beam Sputtering

V. A. Terekhov*, D. S. Usol'tseva, O. V. Serbin, I. E. Zanin, T. V. Kulikova, D. N. Nesterov, K. A. Barkov, A. V. Sitnikov, S. K. Lazaruk, and E. P. Domashevskaya

Voronezh State University, Voronezh, Russia

**e-mail: ftt@phys.vsu.ru*

Received June 14, 2017

Abstract—The peculiarities of the phase composition and electronic structure of aluminum–silicon composite films near the $Al_{0.75}Si_{0.25}$ composition obtained by the magnetron and ion-beam sputtering methods on a Si(100) silicon substrate are studied using the X-ray diffraction techniques and ultrasoft X-ray emission spectroscopy. In addition to silicon nanocrystals of about 25 nm in size, an ordered solid solution corresponding to the previously unknown Al_3Si phase is formed in magnetron sputtering on a polycrystalline Al matrix. Films obtained by ion-beam sputtering of the composite target are found to be monophasic and contained only one phase of an ordered solid solution of aluminum silicide Al_3Si of the *Pm*3*m* cubic system with the primitive cell parameter a = 4.085 Å. However, subsequent pulsed photon annealing of the composite with different radiation doses from 145 to 216 J/cm^2 gives rise to the partial decomposition of the Al_3Si phase with the formation of free metallic aluminum and silicon nanocrystals with sizes in the range from 50 to 100 nm, depending on the pulsed photon radiation dose.

DOI: 10.1134/S1063783418050311

INTRODUCTION

The formation of silicon nanocrystals by different methods in dielectric, semiconductor, and metal matrices with different electrophysical properties allows one to obtain composite materials with new multifunctional optical, electrophysical, and mechanical properties [1].

Among this manifold, aluminum alloys and composites with silicon (silumines) are widely used in various fields of technology, and their mechanical properties strongly depend on the size of silicon crystals that are present in the aluminum matrix. Therefore, the development of a technology for the production of such composites with crystal sizes of about a few dozen nanometers can provide substantial enhancement in these properties.

We have established in [2] that silicon nanocrystals in the $Al_{1-x}Si_x$ composite films obtained by magnetron sputtering with a silicon content of 30 and 45 at % have comparable mean sizes of 20 and 25 nm. Upon the selective etching of aluminum from the composite, the remaining silicon forms a spongy structure in the form of fused conglomerates comprised of silicon nanocrystals.

The aluminum–silicon phase-equilibrium diagram shows [3] that bulk silumin alloys in the hypereutectic region of the compositions should contain solid solutions of silicon in aluminum, and a crystalline silicon phase. In addition, there is a map of the $Al_{3.21}Si_{0.47}$ metastable silicon aluminide phase in the registry of the International Center for Diffraction Data [4], in which the set of interplanar distances contains values that are close to silicon and aluminum, with the strongest reflection of this phase corresponding to d = 2.3432 Å. Moreover, a metastable phase with a simple cubic lattice and a lattice parameter of a = 6.975 Å was reported in [5], which is produced upon superfast cooling of the $Al_{0.80}Si_{0.20}$ melt containing 20% of silicon.

In our previous work [2], we focused on the formation of silicon nanocrystals in magnetron composite films, while the formation of ordered solid solutions or new phases under nonequilibrium conditions was not considered. In the meantime, the energy of particles hitting the substrate during magnetron sputtering equals several electron volts, so the formation of both solid solutions and intermetallic metastable phases is possible even without heating the substrate additionally. Therefore, the present work is devoted to detailed investigation of the phase composition and electronic structure in the Al–Si composite films near the

$Al_{0.75}Si_{0.25}$ composition obtained not only by magnetron sputtering but also by ion-beam deposition.

EXPERIMENTAL

Films of the $Al_{0.73}Si_{0.27}$ composition on a Si(100) silicon substrate were obtained in the Belarusian State University of Informatics and Radioelectronics by magnetron sputtering of a composite target on an Oratoriya-29 system [6]. Films of approximately the same composition ($Al_{0.75}Si_{0.25}$) were obtained in the Voronezh Technical University on similar Si(100) substrates by ion-beam deposition in the chamber with an argon pressure of 8.0×10^{-4} mm Hg, a plasma current of 170 mA, and a voltage of 3500 V [7]. Next, the samples obtained by ion-beam deposition were exposured to pulsed photon annealing (PPA) on a UOLP-1M setup using xenon lamps with a wavelength in the range from 200 to 1200 nm. The film thickness in both cases was about 0.5 μm.

The morphology of the films and their elemental composition were studied on a JEOL JSM-6380LV scanning electron microscope in the Center for Collective Usage of Scientific Equipment of the Voronezh State University. The X-ray diffraction (XRD) phase analysis was carried out using a PANanalytical Empyrean X-ray diffractometer with a Cu$K_{\alpha1}$ radiation source in the same Center for Collective Usage.

The electronic structure of the valence band of the Al–Si thin-film composites was analyzed on a RSM-500 laboratory ultra-soft X-ray spectrometer-monochromator based on the energy distribution of the local partial density of valence states of silicon and aluminum [5, 8]. The emission X-ray Si $L_{2,3}$ spectra were obtained by excitation with electrons of an energy of 3 keV, which corresponds to an analysis depth of 60 nm [9–11].

RESULTS AND DISCUSSION

Diffractometric Studies of the Phase Composition

The results of diffractometric studies of the Al–Si film composites, which are given in Fig. 1 and Table 1, show the following: reflexes of the crystalline phases of aluminum and silicon (curve *3* in Fig. 1) are observed in the $Al_{0.73}Si_{0.27}$ film obtained by magnetron sputtering, the same as in [2]; in addition, a detailed analysis of the XRF data shows the presence of additional reflexes that belong to neither silicon nor aluminum, which are marked in circles in Fig. 1 and correspond to interplanar distances of d = 4.09; 2.04; and 1.67 Å. They are given in Table 1 as belonging to an unknown phase.

Only the reflexes of the same unknown phase are present on the X-ray diffraction pattern of the $Al_{0.75}Si_{0.25}$ composite obtained by ion-beam sputtering, while silicon and aluminum reflexes are absent.

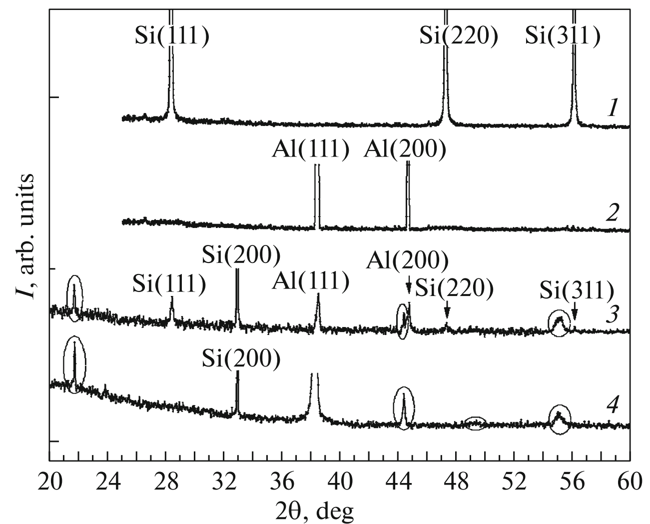

Fig. 1. Diffraction patterns of the reference samples of (*1*) polycrystalline silicon and (*2*) polycrystalline aluminum, and of the samples obtained by (*3*) magnetron sputtering and (*4*) ion-beam deposition.

The most intense reflex close to the Al(111) reflex also belongs, as is shown below, to the phase, which we call "the unknown phase" tentatively.

The Si(200) reflex, which is present on the diffraction patterns of both films (curves *3* and *4* in Fig. 1) and absent in the diffraction pattern of poly-Si, arises from the weak forbidden reflection on the single-crystal Si(100) substrate as the second-order reflection. Since the X-ray microanalysis showed that this composite contains about 25 at % of silicon and 75 at % of aluminum, the absence of four silicon and aluminum reflexes in the X-ray diffraction pattern *4*, besides the strongly shifted Al(111) reflex, may indicate that either the entire atomized material is included into the composition of the unknown phase or some phases are in an amorphous state.

Density Distribution of Electron States in the Valence Band of Film Composites According to the Ultrasoft X-Ray Spectroscopic Data

To investigate the composites with possible amorphous components, we used the method of ultrasoft X-ray emission spectroscopy (USXRES), which perfectly reflects the distribution of the local partial density of electron states in the valence band of both crystalline and amorphous phases. The Si $L_{2,3}$ spectra of these film composites were obtained on an RSM-500 spectrometer, which reflect the distribution of the Si 3*s*, *d* states in the valence band [8, 9]. In the case of ion-beam deposition of Al–Si composites, the comparison of the resulting data given in Fig. 2 (the energy scale with respect to the Si 2*p* level) with the Si $L_{2,3}$ spectra of the reference (curve *1*) *c*-Si and (curve *2*)

Table 1. Interplanar spacings in the reference samples of polycrystalline silicon and polycrystalline aluminum, and in the initial samples of film composites obtained by magnetron and ion-beam deposition methods (according to X-ray diffraction data in the angular range $2\theta = 20°–60°$)

Nos.	Interplanar spacings (Å) corresponding to X-ray reflexes given in Fig. 1				Phase assignment
	poly-Si	poly-Al	sample obtained by magnetron sputtering	sample obtained by ion-beam sputtering	
1	–	–	4.09	4.09	Unknown phase
2	3.14	–	3.14	–	Si(111)
3	–	–	2.72	2.72	Si(200) substrate
4	–	2.33	2.34	–	Al(111)
				2.35	Unknown phase
5	–	–	2.04	2.04	Unknown phase
6	–	2.02	2.02	–	Al(200)
7	1.92	–	1.92	–	Si(220)
8	–	–	–	1.85	Unknown phase
9	–	–	1.67	1.67	Unknown phase
10	1.638	–	1.63	–	Si(311)

a-Si samples showed that the distribution (curve *4*) of the Si 3*s*, *d* states of silicon in this particular composite with the $Al_{0.75}Si_{0.25}$ composition differs from the first two spectra by the presence of one density maximum at ~91 eV, which is attributed to a single crystalline phase (unidentified yet), which is present in this composite containing both silicon and aluminum. At the same time, two pronounced maxima of the density of states of nanocrystalline silicon at 89.5 and 92.0 eV are observed in the Si $L_{2,3}$ spectrum of the film obtained by magnetron sputtering (curve *3* in Fig. 2), which are attributed to the first two valence subbands of silicon. The influence of the unknown phase is manifested in equalization of the intensity of these two maxima in the composite, whereas the main maximum in the crystalline silicon is positioned at 92.0 eV (curve *1* in Fig. 2).

The obtained USXRES results explain why the reflexes of nanocrystalline silicon are detected on the X-ray diffraction pattern of the composite obtained by magnetron sputtering, whereas the reflexes of crystalline silicon (except for one substrate reflex), as well as the reflexes of crystalline aluminum, are not observed on the X-ray diffraction pattern of the composite obtained by ion-beam deposition (Fig. 1). This is due to the formation of a new unknown phase on the monocrystalline substrate in the Al–Si system, the chemical formula of which should correspond to the composition of the ordered $Al_{0.75}Si_{0.25}$ solid solution, i.e., to the aluminum silicide Al_3Si.

A similar result was obtained in the studies [12] when the process of magnetron sputtering of a target of the appropriate composition yields a single-phase condensate of the ordered $Pd_{0.5}Cu_{0.5}$ solid solution with a primitive cubic crystal lattice of the CsCl type (β phase).

According to the estimates of the authors of [12], the temperature of the unheated substrate during its growth can increase from the initial temperature (about 300 K) by 50–100 K as a result of the high energy of condensed atoms and the influence of plasma components.

In order to check the stability of the Al_3Si phase and the possibility of formation of silicon nanocrystals in such a film condensate, the film samples obtained by ion-beam deposition were exposed to pulsed photon annealing with radiation doses in the range from 145 to 215 J/cm^2. PPA was performed in a vacuum of $\sim 10^{-5}$ mm Hg for a few seconds in order to minimize the oxidation of silicon and aluminum in the residual air atmosphere.

The Si $L_{2,3}$ spectra of these composites after annealing with different irradiation doses are shown in Fig. 3. The analysis of the shapes of the spectra shows that annealing at 145 J/cm^2 leads to the emergence of a main maximum of the density of silicon *s*-states at an energy of 92 eV, which is typical for the crystalline *c*-Si (Fig. 2) and nanocrystalline *nc*-Si silicon [2], as well as to the appearance of a shoulder in the range 89–91 eV (curve *1* in Fig. 3). The presence of these structures evidences the generation of nanocrystalline silicon in the composite after PPA. At the same time, the absence of a clear sink between two maxima of the density of states at $h\nu \approx 91$ eV, as is observed in *c*-Si and *nc*-Si, i.e., a clearly expressed fine structure of the density of states in the main part of the valence band, is attributed to the influence of the Al_3Si phase that is not completely decomposed after PPA.

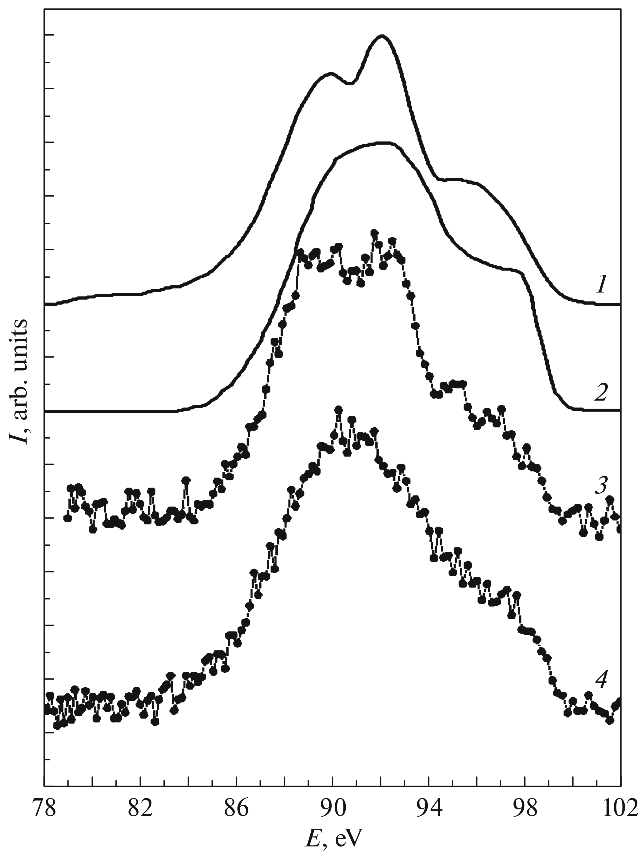

Fig. 2. X-ray emission Si $L_{2,3}$ spectra of the reference samples of (*1*) crystalline and (*2*) amorphous silicon and of the samples obtained by (*3*) magnetron sputtering and (*4*) ion-beam deposition.

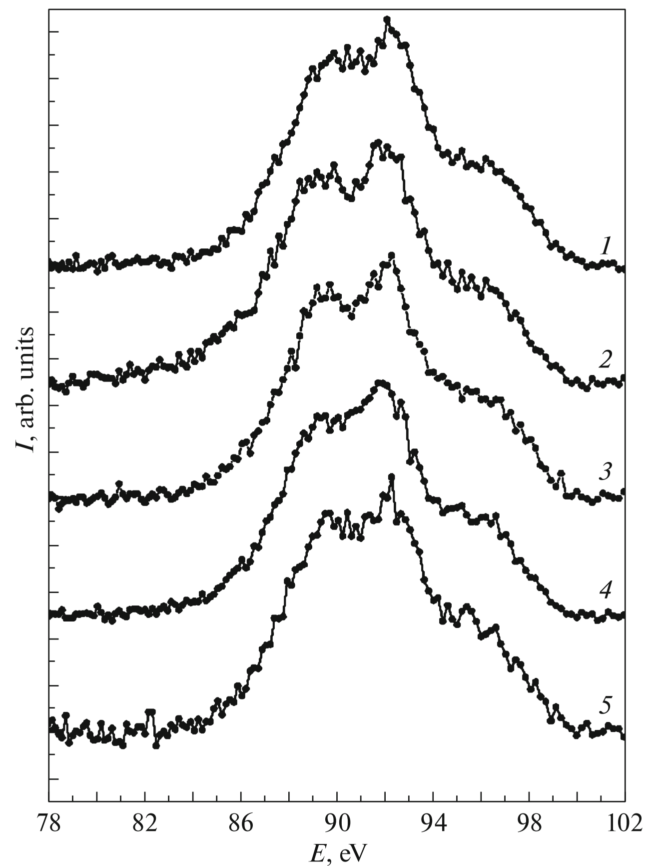

Fig. 3. Ultrasoft X-ray emission Si $L_{2,3}$ spectra of the samples obtained by ion-beam deposition after the exposure to PPA with doses of (*1*) 145, (*2*) 150, (*3*) 160, (*4*) 180, and (*5*) 216 J/cm^2.

An increase in the PPA dose to 150 and 160 J/cm^2 gives rise to an increase in the influence of nanocrystalline silicon on the Si $L_{2,3}$ spectra of irradiated composites, which become more and more akin to the spectra of *nc*-Si (curves *2* and *3* in Fig. 3), but the influence of the Al_3Si phase is still retained even after a further increase in the PPA dose up to 180 and 216 J/cm^2.

The ultrasoft X-ray emission Al $L_{2,3}$ spectra of these same composites before and after PPA with different doses are shown in Fig. 4. The lower curve in Fig. 4 corresponds to metallic aluminum. The convex semiparabolic curve of the dependence of the density of states on the energy in the first filled and second half-filled electronic bands of Al is well described in the approximation of nearly free electrons. The sharp high-energy edge of the emission band corresponds to the position of the Fermi level in the metal. The above placed Al $L_{2,3}$ spectrum, which is related to the initial unannealed $Al_{0.75}Si_{0.25}$ sample with a lone crystalline Al_3Si phase, differs significantly from the previous spectrum of the metal and is described by a semi-parabolic curve concave with respect to the energy scale. The further analysis of the shape of the spectra of the samples after PPA with different doses shows a gradual increase in the intensity of the spectrum near the first zone and the approaching of its shape to the spectrum of the metal due to an increase in the part of the Al_3Si phase that has decayed into aluminum and silicon.

X-Ray Diffraction Studies of the $Al_{0.75}Si_{0.25}$ Samples Obtained by the Method of Ion-Beam Deposition after the Exposure to PPA

The X-ray diffraction studies of the same $Al_{0.75}Si_{0.25}$ samples after their exposure to PPA showed (Fig. 5 and Table 2) that a PPA dose of 145 J/cm^2 gives rise to the emergence of three reflexes of the nanocrystalline silicon phase, namely, the Si(111), Si(220), and Si(311) reflexes that are sufficiently weak and broad.

With an increase in the annealing dose to 150–160 J/cm^2, the intensity of silicon reflexes increases and then decreases upon an increase in the PPA dose to 180–216 J/cm^2. This effect may indicate partial decay of the Al_3Si crystal phase in the course of fast

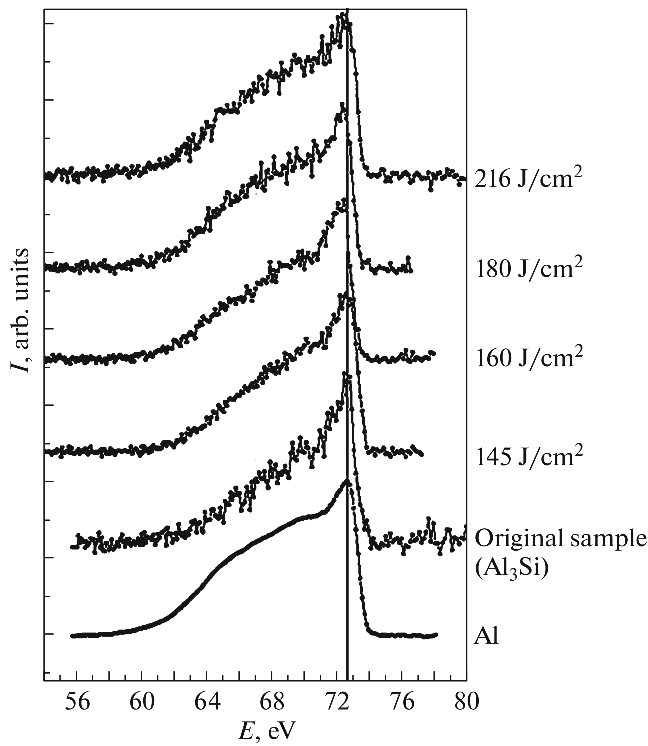

Fig. 4. X-ray emission Al $L_{2,3}$ spectra of the samples obtained by ion-beam deposition before and after the exposure to PPA in different doses.

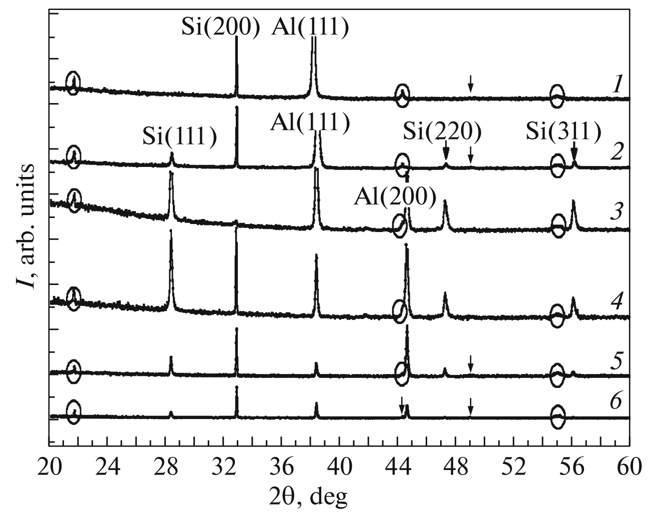

Fig. 5. Diffraction patterns of the samples obtained by ion-beam deposition (*1*) before and after the exposure to PPA with doses of (*2*) 145, (*3*) 150, (*4*) 160, (*5*) 180, and (*6*) 216 J/cm^2; the circles show the reflexes from an unknown phase.

melting of the film under a more powerful PPA flow and subsequent cooling, which gives rise to the formation of silicon and aluminum nanocrystalline phases (Fig. 5 and Table 2).

An estimate of the average size of silicon nanocrystals from the broadening of the reflexes by the Debye–Scherrer formula gives a value of about 50 nm at annealing doses of 145–160 J/cm^2 and up to about 100 nm at doses of 180–216 J/cm^2.

The intensity of the aluminum Al(111) and Al(200) reflexes that are absent in the initial composite varies nonmonotonically with an increase in the PPA dose, it suddenly decreases and then increases (see Fig. 5), which is connected, apparently, with the rearrange-

Table 2. Interplanar spacings in the samples of film composites obtained by ion-beam sputtering before and after PPA at different radiation doses (according to the X-ray diffraction data in the angular range 2θ = 20°–60°)

No.	Interplanar spacings (Å) corresponding to X-ray reflexes given in Fig. 4						Phase assignment
	before PPA	after PPA 145 J/cm^2	after PPA 150 J/cm^2	after PPA 160 J/cm^2	after PPA 180 J/cm^2	after PPA 216 J/cm^2	
1	4.09	4.08	4.09	4.09	4.08	4.08	Unknown phase
2	–	3.13	3.14	3.14	3.14	3.14	Si(111) (*nc*)
3	2.72	2.72	2.72	2.72	2.72	2.72	Si(200) substrate
4	–	2.34	2.34	2.34	2.34	2.34	Al(111)
5	2.35	–	–	–	–	–	Unknown phase
6	2.04	2.04	2.04	2.04	2.04	2.04	Unknown phase
7	–	–	2.03	2.03	2.03	2.03	Al(200)
8	–	1.92	1.92	1.92	1.92	1.92	Si(220) (*nc*)
9	1.85	1.86	–	–	1.85	1.86	Unknown phase
10	1.67	1.67	1.67	1.67	1.67	1.67	Unknown phase
11	–	1.63	1.64	1.64	1.64	1.64	Si(311) (*nc*)

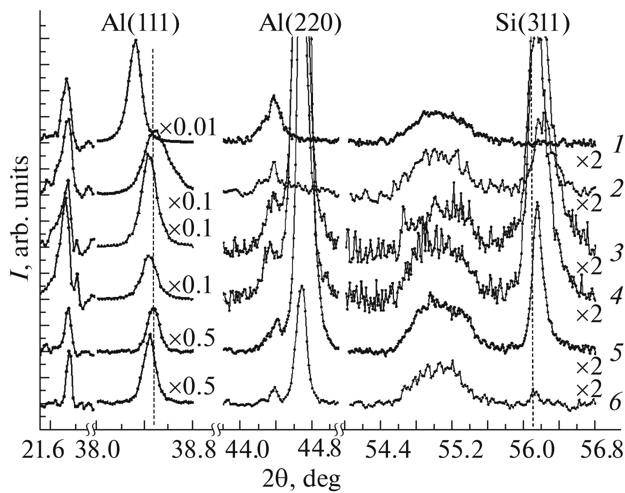

Fig. 6. Diffraction patterns of the samples obtained by ion-beam deposition (*1*) before and after the exposure to PPA with doses of (*2*) 145, (*3*) 150, (*4*) 160, (*5*) 180, and (*6*) 216 J/cm^2 in the region of "extra" reflexes and the Al(111), Al(200), and Si(311) reflexes; the discontinuous line shows the position of the Al(111) and Si(311) reflexes in the reference polycrystalline aluminum and silicon samples.

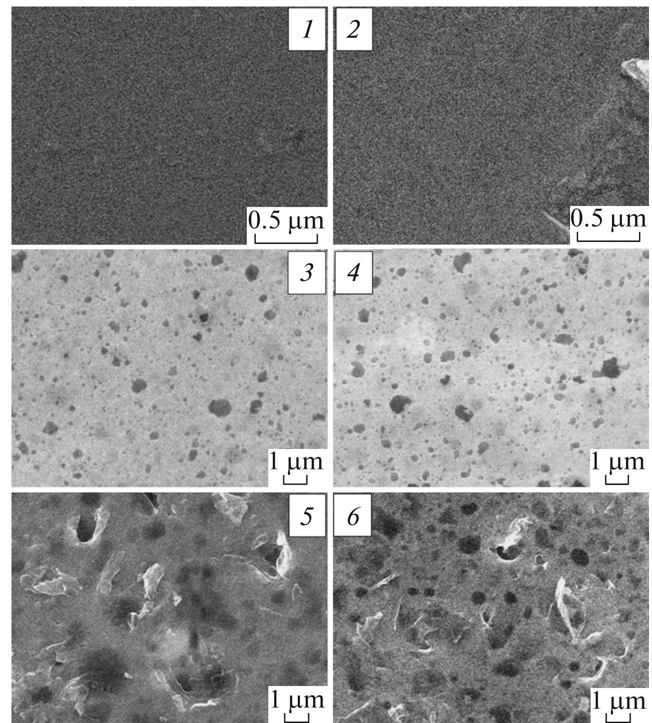

Fig. 7. Scanning electron microscopy images of the samples obtained by ion-beam deposition (*1*) before and after the exposure to PPA with doses of (*2*) 145, (*3*) 150, (*4*) 160, (*5*) 180, and (*6*) 216 J/cm^2.

ment of the mutual alignment of microcrystals and the texturing processes in the film.

Next, let us analyze in more detail the effect of PPA on the behavior of the Al_3Si phase reflexes in the $Al_{0.75}Si_{0.25}$ composites obtained by ion-beam deposition. The sections of the X-ray diffraction pattern, on which the reflections of this phase are observed, are shown in Fig. 6. In addition, the aluminum Al(111) and Al(200) reflexes and the silicon S(311) reflex are shown in this figure. The positions of the Al(111) and Si(311) reflexes in the reference polycrystalline silicon and aluminum samples are marked by discontinuous vertical lines. In addition to the noticeably shifted diffraction patterns show additional reflexes $d = 4.09$ Å in addition to the noticeably shifted Al(111) and Al(200) reflexes with $d = 2.35$ Å and $d = 2.04$ Å, respectively, which are related to the Al_3Si phase, extra reflexes belonging to the same phase are observed at $d = 4.09$ Å ($2\theta = 21.74°$) and $d = 1.67$ Å ($2\theta = 55.02°$) in the X-ray diffraction pattern of the film obtained by ion-beam deposition. A reflex of nanocrystalline silicon and an influx from the Al(200) reflection appear on the right side from the line $d = 2.04$ Å of the Al_3Si phase upon annealing with a dose of 145 J/cm^2 (curve *2* in Fig. 6). The annealing with doses of 150, 160, and 180 J/cm^2 gives rise to the appearance of not only a strong Si(311) reflex of silicon but also a very intense Al(200) reflex at the position $d = 2.02$ Å corresponding to polycrystalline aluminum; as a result, two reflexes are present in the X-ray diffraction pattern, one of which ($d =$ 2.04 Å) corresponds to the Al_3Si phase and the second one (with $d = 2.02$ Å) corresponds to aluminum. Both these reflexes remain even after more powerful annealing, but their relative intensities are different in this case (see Fig. 6).

The Al(111) reflex behaves somewhat differently during the PPA process. In the initial film, the interplanar spacing equaling $d = 2.35$ Å is increased in comparison with pure aluminum and corresponds to the Al_3Si phase. After annealing at 145 J/cm^2, the reflex shifts towards larger angles by about 0.3° and becomes wider ($\Delta\theta \approx 0.30°$), but again becomes narrower ($\Delta\theta \approx 0.11°$) after annealing with a dose of 150 J/cm^2. At high PPA doses, the position of the Al(111) reflex does not change and corresponds to pure Al (Fig. 6).

As is seen from Fig. 6, a Si(311) reflex of nanocrystalline silicon appears simultaneously with reflexes of crystalline aluminum in all the annealed composites irrespective of the annealing conditions, the relative intensity of which changes synchronously with the relative intensity of the Al(200) reflex, which once again confirms their origin as a result of the partial decomposition of the Al_3Si phase under the influence of PPA.

The data of scanning electron microscopy indicate the possibility of such a rearrangement (Fig. 7). There are no pronounced heterogeneities on the film surface before the exposure to PPA and after PPA with a dose

Table 3. Theoretically calculated and experimental values of the interplanar spacings in the ordered $Al_{0.75}Si_{0.25}$ solid solution (silicide Al_3Si) with a primitive unit cell of the cubic syngony *Pm*3*m* and a lattice parameter of 4.085 Å

hkl	Theoretically calculated interplanar spacing values *d* (Å) for planes with indices (*hkl*)	Experimental interplanar spacings values *d* (Å) for initial sample obtained by ion-beam sputtering	Experimental values of absolute (number of pulses per second) and relative (%) intensities of X-ray diffraction lines
100	4.085 (001)	4.085	259 (5.2%)
110	2.885 (110)	–	–
111	2.356 (111)	2.352	4993 (100%)
200	2.040 (200)	2.040	158 (3.2%)
210	1.825 (210)	1.847	24 (0.5%)
211	1.666 (211)	1.668	67 (1.3%)

of 145 J/cm^2. After PPA with doses of 150–160 J/cm^2, numerous submicron-sized inhomogeneities appear on the film surface. A further increase in the annealing dose to 180–216 J/cm^2 is accompanied by the emergence of larger inhomogeneities.

Type and Parameters of the Crystal Structure of the Al_3Si Phase

Thus, all the previous data of the X-ray diffraction and X-ray spectroscopy studies convince us that silicon interacting with aluminum under the nonequilibrium conditions of both the ion-beam and magnetron sputtering of a composite target forms an ordered solid solution of the $Al_{0.75}Si_{0.25}$ composition corresponding to the Al_3Si aluminum silicide phase with the following set of interplanar distances given in Table 3: 4.085, 2.352, 2.040, 1.847, and 1.668 Å. This set of interplanar distances corresponds to a primitive type of a unit cell of the cubic syngony *Pm*3*m* with a lattice parameter of a = 4.085 Å. The crystalline structure of the compound Al_3Si can be represented by four primitive cubic sublattices, one of which is comprised of silicon atoms and three others formed by aluminum atoms are shifted with respect to the former to distances of (1/2; 0; 0), (0; 1/2; 0), and (0; 0; 1/2) in the lattice parameter units. The calculated set of interplanar spacings with appropriate crystallographic plane indices, which are given in the first column of Table 3, corresponds to this lattice parameter a = 4.085 Å.

Reflexes corresponding to the interplanar spacings that are close to the calculated values are observed in the experiment (Table 3), with the exception of the reflex at d = 2.88 Å. Even under the signal accumulation mode, we were not able to register this reflex; this may be connected with its extremely low relative intensity.

CONCLUSIONS

Thus, the results of the investigation of the phase composition and the local partial density distribution of states in the valence band of thin Al–Si films, obtained by ion-beam and magnetron sputtering and containing 23–25 at % of silicon, show that their phase composition may differ in the presence or absence of silicon nanocrystals, depending on the method and conditions, at which the films are formed. In addition to the phases of crystalline aluminum and nanocrystalline silicon with an average grain size of about 25 nm, the composite films obtained by magnetron sputtering include the phase of an ordered solid solution of Al_3Si with the cubic lattice *Pm*3*m* and a lattice parameter of a = 4.085 Å. At the same time, only the Al_3Si phase is present in the initial $Al_{0.75}Si_{0.25}$ films obtained by ion-beam sputtering. Pulsed-photon annealing of these films leads to a partial decay of the Al_3Si phase with the formation of metallic aluminum and nanocrystalline silicon in the composition. The size of silicon nanocrystals is 50–100 nm and depends on the annealing conditions.

ACKNOWLEDGMENTS

This work was supported by the Ministry of Education and Science of the Russian Federation within the State Assignment for Universities in the Field of Scientific Activity for 2017–2019 (project no. 3.6263.2017/VU).

REFERENCES

1. *Nanotechnology Research Directions: Vision for Nanotechnology in the Next Decade*, Ed. by M. C. Roco, S. Williams, and P. Alivisatos (Springer, Dordrecht, 2000).
2. V. A. Terekhov, S. K. Lazaruk, D. S. Usol'tseva, A. A. Leshok, P. S. Katsuba, I. E. Zanin, D. E. Spirin, A. A. Stepanova, and S. Yu. Turishchev, Phys. Solid State **56**, 2543 (2014).

3. *State Diagrams of Binary Metallic Systems*, Ed. by N. P. Lyakishev (Moscow, Mashinostroenie, 1996) [in Russian], Vol. 1.
4. JCPDS—International Centre for Diffraction Data, PCPDFWIN, Vol. 22, card No. 41-1222.
5. A. K. Kushnereva and I. V. Salli, Neorg. Mater. **6**, 1867 (1970).
6. S. K. Lazorouk, A. A. Leshok, V. A. Labunov, and V. E. Borisenko, Semiconductors **39**, 136 (2005).
7. Yu. E. Kalinin, A. V. Sitnikov, O. V. Stognei, I. V. Zolotukhin, and P. V. Neretin, Mater. Sci. Eng. **304–306**, 941 (2001).
8. T. M. Zimkina and V. A. Fomichev, *Ultrasoft X-Ray Spectroscopy* (Leningr. Gos. Univ., Leningrad, 1971) [in Russian].
9. V. V. Nemoshkalenko and A. G. Aleshin, *Theoretical Principles of X-Ray Emission Spectroscopy* (Naukova Dumka, Kiev, 1974) [in Russian].
10. A. S. Shulakov and A. P. Stepanov, Poverkhnost’, Fiz. Khim. Mekh., No. 10, 146 (1988).
11. V. A. Terekhov, S. N. Trostyanskii, A. E. Seleznev, and E. P. Domashevskaya, Poverkhnost’. Fiz. Khim. Mekh., No. 5, 74 (1988).
12. V. M. Ievlev, A. A. Maksimenko, S. V. Kannykin, A. I. Dontsov, K. A. Solntsev, E. K. Belonogov, and N. R. Roshan, Dokl. Phys. Chem. **457**, 127 (2014).

Translated by O. Kadkin